Acoustic metamaterials with circular sector cavities and programmable densities

W. Akl and A. Elsabbagh
Faculty of Engineering, Ain Shams University, Cairo, 11517, Egypt

A. Baz
Mechanical Engineering Department, University of Maryland, College Park, Maryland 20742

(Received 6 July 2011; revised 23 April 2012; accepted 26 April 2012)

Considerable interest has been devoted to the development of various classes of acoustic metamaterials that can control the propagation of acoustical wave energy throughout fluid domains. However, all the currently exerted efforts are focused on studying passive metamaterials with fixed material properties. In this paper, the emphasis is placed on the development of a class of composite one-dimensional acoustic metamaterials with effective densities that are programmed to adapt to any prescribed pattern along the metamaterial. The proposed acoustic metamaterial is composed of a periodic arrangement of cell structures, in which each cell consists of a circular sector cavity bounded by actively controlled flexible panels to provide the capability for manipulating the overall effective dynamic density. The theoretical analysis of this class of multilayered composite active acoustic metamaterials (CAAMM) is presented and the theoretical predictions are determined for a cascading array of fluid cavities coupled to flexible piezoelectric active boundaries forming the metamaterial domain with programmable dynamic density. The stiffness of the piezoelectric boundaries is electrically manipulated to control the overall density of the individual cells utilizing the strong coupling with the fluid domain and using direct acoustic pressure feedback. The interaction between the neighboring cells of the composite metamaterial is modeled using a lumped-parameter approach. Numerical examples are presented to demonstrate the performance characteristics of the proposed CAAMM and its potential for generating prescribed spatial and spectral patterns of density variation. © *2012 Acoustical Society of America*. [http://dx.doi.org/10.1121/1.4744936]

PACS number(s): 43.40.At, 43.40.Fz, 43.50.Fe [ANN] Pages: 2857–2865

I. INTRODUCTION

Metamaterials, either acoustic or electromagnetic, have recently attracted the focus of many researchers as a new technique for achieving wave propagation patterns, which are impossible to realize using regular composite materials.[1–3] Developing acoustic or electromagnetic metamaterials is physically analogous to engineering periodic material structure using the inclusions of small inhomogeneities to enact effective macroscopic behavior.[4] Acoustic metamaterials are therefore considered as those material structures, rather than compositions, that are designed and artificially fabricated to control, guide, and manipulate sound in the form of sonic, infrasonic, or ultrasonic waves, as these might occur in gases, liquids, and solids. The hereditary line into acoustic metamaterials follows from the theory and research in electromagnetic metamaterials as first developed by Pendry[5] who has proven that using negative refractive index would result in a perfect lens. In 2006, Pendry *et al.*[6] were the first to present the transformation-based solutions to the Maxwell's equations, which have proven to yield a general method for rendering arbitrarily sized and shaped objects electromagnetically invisible. This was based on the invariance of the Maxwell's equations under coordinate transformation.[7,8] Further, with acoustic metamaterials, sonic waves can now be extended to the negative refraction domain[9].

Control of various forms of sonic waves mostly requires controlling of the bulk modulus B and the density ρ, which are counterparts to the electromagnetic permittivity and permeability. The speed of sound, on the other hand, being totally dependent on B and ρ, is analogous to the refractive index in electromagnetic domain. It is therefore due to the analogy to the wave equation in electromagnetic, researchers have developed the theoretical foundation of acoustic metamaterials,[10,11] where their focus was directed toward various wave propagation control applications with special interest in acoustic cloaking rendering objects acoustically invisible.

Several attempts to theoretically and physically control the bulk modulus and density of different material compositions and structures have been reported, aiming eventually at controlling the acoustic wave propagation. On the path to control the bulk modulus, two approaches have been reported in literature; the first was by combining two different isotropic materials in a composite pattern to yield anisotropic properties that can influence the spatial wave propagation patterns.[12–14] In the second mechanism, acoustic impedance mismatch is introduced along the path of wave propagation by integrating flexible sections into the rigid-walled waveguides in order to vary the speed of sound and effective bulk modulus at these sections.[15–17] Manipulation of the material density, on the other hand, has also been reported using two different approaches; the first was by combining two different materials with different densities in a specific spatial arrangement that would yield a homogenized value of the density all over the domain. Such an approach was adopted by[18–20] using phononic crystals. In

the second approach, the concept of dynamic density, which depends on the neighboring material stiffness, was implemented. This approach was manifested in the attempts of synthesizing prescribed dynamic acoustic densities in fluid domains by introducing lattice systems of mass-in-mass units.[21–24] These attempts merely focused on introducing negative effective density motivated by the mathematical analogy between acoustic and electromagnetic waves, where the theoretical possibility of having negative electromagnetic permittivity and permeability was introduced by Pendry.[5]

In all these studies the focus has been placed on passive metamaterials with fixed material properties, which has considerably limited the applicability of this new generation of structured metamaterials in wave propagation control due to the narrow operating bandwidth in the vicinity of the internal cell structure resonances. Very few researchers have tackled the idea of having programmable material properties (bulk modulus and/or density). Baz[25,26] studied the concept of theoretically realizing programmable density using a periodic structure that contains actively controlled piezoelectric elements coupled with fluid domain to control the effective dynamic density in the composite structure. Akl and Baz[27] have also applied the same concept in controlling the effective bulk modulus of the composite domain. In their development, the authors have, however, limited their model to straight one-dimensional structures. In this paper, the emphasis is placed on the development of a new class of one-dimensional composite circular sector-type acoustic metamaterials with tunable effective densities, which can be tailored to have increasing or decreasing variation along the material volume. Due to the proposed geometry, which is more oriented toward applications involving cylindrical domains such as acoustic cloaking for example, the wave fronts introduced follow the same physics of two-dimensional circular waves, such as amplitude dependence on the radial distance from the sound source. Such dependence introduces more complexity in calculating the acoustic-electrical circuit analogy manifested in the expressions of the capacitors and inductors representing the fluid domain compliance and mass, respectively, which to the authors' knowledge has not been treated yet. A piezoelectric sector element coupled with a circular sector acoustic cavity is introduced to form a homogenized periodically structured sector-shaped acoustic metamaterial. The effective dynamic density is controlled using the piezoelectric ingredient in the composite structure. A detailed theoretical analysis is introduced to present a lumped-parameter model of the developed metamaterial. Acoustic-electrical circuit analogy is used to model the cavity characteristics, as this approach has proven to be effective, provided the overall dimensions of the cavity are much smaller than the wavelengths of the acoustic waves passing through. A set of cascading "cells" of the developed metamaterial cell is also introduced showing the capability of such configuration to control the densities along the path of the wave propagation. In addition, the necessary precautions to eliminate the instabilities are introduced. These instabilities occur in the piezoelectric element due to the active control that might exceed the buckling limit leading to entire damage in the integrity of the composite metamaterial structure.

II. ELECTRIC ANALOGY OF CIRCULAR SECTOR ACOUSTIC CAVITIES

In order to derive the acoustic-electric circuit analogy to circular sector acoustic cavities, a brief summary of the acoustic-electric straight cavity is introduced. Euler and continuity equations are presented, which are later implemented in modified form to capture the divergence effect of the cavity cross section on the wave equation in sector acoustic cavities.

A. Straight cavity

A straight acoustic cavity with uniform cross-sectional area A_{st} and length l_f, subject to acoustic pressure drop Δp resulting in volumetric flow rate dQ, is considered. The fluid considered inside the cavity is characterized with static fluid density ρ_f and bulk modulus B_f. The value of dQ depends on three major forces; inertia forces due to the mass of the fluid inside the cavity, elastic forces due to the "stiffness" of the entrapped fluid volume, and finally friction and damping forces, which are ignored in the current analysis.

1. Inertia forces

Newton's second law necessitates that the net force due to the pressure difference Δp equals the rate of change of fluid momentum as given by

$$A_{st}\Delta p = \rho_f l_f A_{st}\frac{dv}{dt}, \tag{1}$$

where v is the particle velocity. For a uniform velocity along the cavity length, $dQ/dt = A_{st}(dv/dt)$, the inertial impedance of the straight cavity after Laplace transformation is given by

$$\frac{\Delta P(s)}{Q(s)} = \frac{\rho_f l_f}{A_{st}}s = L_F s = Z_{LF}(s). \tag{2}$$

2. Elastic forces

The second type of forces is due to the stiffness of the fluid domain. A pressure drop of Δp across the cavity will cause the fluid to be "strained" due to change in its volume Vol by an amount of $d(\text{Vol})$ such that $\varepsilon_V = -d(\text{Vol})/\text{Vol}$, and as the bulk modulus B_f is defined as the difference in pressure, which yields a unit volume strain, $\Delta p = -B_f\, d(\text{Vol})/\text{Vol}$. The change in volume $d(\text{Vol})$ along a period of time dt is defined as: $d(\text{Vol}) = -\int Q\, dt$. Hence, and applying Laplace transformation to Δp, the elastic and total impedance for the straight acoustic cavity Z_{CF} and Z_t are calculated as

$$Z_{CF}(s) = \frac{\Delta P(s)}{Q(s)} = \frac{1}{C_F s} = \frac{1}{s}\frac{B_f}{A_{st}l_f} \tag{3}$$

$$Z_t(s) = Z_{LF}(s) + Z_{CF}(s) = \frac{\rho_f l_f s}{A} + \frac{B_f}{A_{st}l_f s}. \tag{4}$$

B. Circular sector acoustic cavity

A sector of the fluid domain with point source and acoustic pressure wave propagating in the radial direction is as shown in Fig. 1(a). The sector cavity shown, expands from $r = r_1$ to $r = r_2$, which includes a central angle γ. A slice of thickness dr is considered for force balance and mass flow rate calculations.

1. Inertia forces

Considering the infinitesimal slice of thickness dr in the sector cavity, Newton's second law necessitates that $A(r)dp = \rho_f A(r)(dv/dt)dr$, where $A(r) = \gamma H r$, H is the cavity depth. As $dQ/dt = A(r)(dv/dt)$ and integrating $(r_1 \rightarrow r_2)$, the inertial impedance term is defined as

$$Z_{LF} = \frac{\Delta P(s)}{Q(s)} = s\frac{\rho_f}{H_\gamma}\ln\frac{r_2}{r_1}, \tag{5}$$

where in the limit case $(\gamma \rightarrow 0)$, Z_{LF} reduces to the form for straight cavity $(\lim_{\gamma\rightarrow 0} Z_{LF}(s) = s(\rho_f(r_2 - r_1)/Hb_1))$, where b_1 is the chord lengths of the inner circular sector.

2. Elastic forces

For sector cavity, a different approach is implemented in order to calculate the effect of the elastic forces on the acoustic cavity as follows:

$$\int_{r_1}^{r_2} F dr = \Delta PE, \tag{6}$$

where F is the elastic force inside the sector cavity and ΔPE is the change in potential energy. Rewriting Eq. (6) such that $\int_{r_1}^{r_2} A(r)Tdr = \Delta p \Delta \mathrm{Vol}$, where $A(r)$ is the cross-sectional area of the sector cavity at radius r, T is the normal stress, Δp is the pressure difference across the sector cavity, and substituting for T with S/S^E, where S is the mechanical strain and s^E is the mechanical compliance, dividing by ΔVol inside the integral and completing the integration while replacing $1/s^E$ with fluid bulk modulus B_f results in

$$\Delta p = \int_{r_1}^{r_2} \frac{A(r)l_f B_f}{H\gamma r l_f^2} dr = \frac{\Delta \mathrm{Vol}\ B_f}{H\gamma l_f^2}\ln\frac{r_2}{r_1} \tag{7}$$

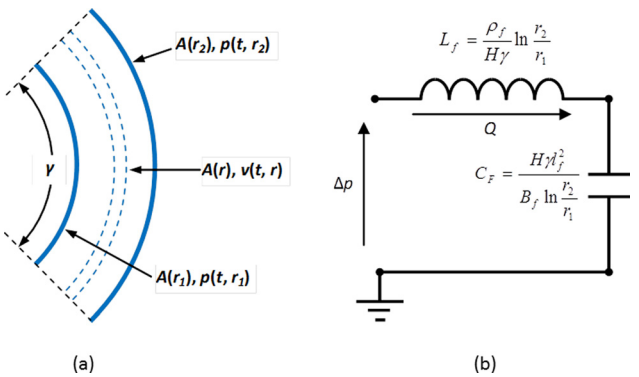

FIG. 1. (Color online) (a) Geometry of the acoustic sector cavity, (b) electric circuit analogous to the acoustic sector cavity.

from which the elastic and total impedances Z_{CF} and Z_t, as shown in Fig. 1(b) are calculated as

$$Z_{CF}(s) = \frac{\Delta P(s)}{Q(s)} = \frac{1}{C_F s} = \frac{1}{s}\frac{B_f}{H\gamma l_f^2}\ln\frac{r_2}{r_1}, \tag{8}$$

$$Z_t(s) = Z_{LF}(s) + Z_{CF}(s) = s\frac{\rho_f}{H\gamma}\ln\frac{r_2}{r_1} + \frac{1}{s}\frac{B_f}{H\gamma l_f^2}\ln\frac{r_2}{r_1}. \tag{9}$$

C. Dynamic density for sector acoustic cavity

Combining both the "inertia" and stiffness impedances and substituting $B_f = \rho_f c_f^2$, where c_f is the speed of sound in the fluid domain, the dynamic equation for the circular sector acoustic cavity is given as

$$\Delta p = -\frac{\rho_f s Q}{H\gamma}\left(\ln\frac{r_2}{r_1} + \frac{c_f^2}{l_f^2}\ln\frac{r_2}{r_1}\frac{1}{s^2}\right). \tag{10}$$

For very small cavities, $(r_2/r_1 = 1 + \alpha, \quad \alpha \ll 1)$ and defining $Q = A_{\mathrm{Ave}} \times \nu$ and ρ_{eff}: $\left(\Delta p/l_f = -\rho_{\mathrm{eff}}(dv/dt)\right)$, the relative density of the acoustic cavity is defined as

$$\frac{\rho_{\mathrm{eff}}}{\rho_f} = \left(\frac{A_{\mathrm{Ave}}}{H\gamma l_f}\ln\frac{r_2}{r_1} + \frac{A_{\mathrm{Ave}}c_f^2}{H\gamma l_f^3 s^2}\ln\frac{r^2}{r_1}\right), \tag{11}$$

which, for a straight cavity, would converge to the form given by Baz.[25]

D. Dynamic density for sector acoustic cavity coupled with flexible diaphragm

Considering a sector acoustic cavity coupled to a flexible diaphragm as shown in Fig. 2(a) with its analogous lumped parameter electric circuit shown in Fig. 2(b), the flexible diaphragm, coupled with the acoustic sector cavity, represents a composite material that consists of two components characterized with different densities (ρ_f, ρ_d), bulk moduli (B_f, B_d), and thicknesses ($l_f = r_2 - r_1$, $l_d = r_3 - r_2$) for the fluid and flexible diaphragms, respectively. Applying electrical circuit analogy to the acoustic cavity, the overall circuit impedance (Z_t) is calculated by summing up the different impedances representing the different inductors and capacitors in the circuit as follows:

$$Z_{LF} = L_F s = \rho_f \frac{1}{H\gamma}\ln\frac{r_2}{r_1}s, \tag{12}$$

$$Z_{LD} = L_D s = \rho_d \frac{1}{H\gamma}\ln\frac{r_3}{r_2}s, \tag{13}$$

$$Z_{CF} = \frac{1}{C_F s} = \frac{1}{s}\frac{B_f}{H\gamma l_f^2}\ln\frac{r_2}{r_1}, \tag{14}$$

$$Z_{CD} = \frac{1}{C_D s} = \frac{1}{s}\frac{B_d}{H\gamma l_d^2}\ln\frac{r_3}{r_2}, \tag{15}$$

$$Z_t = \frac{(Z_{CD} + Z_{LD})Z_{CF}}{Z_{CD} + Z_{LD} + Z_{CF}} + Z_{LF}. \tag{16}$$

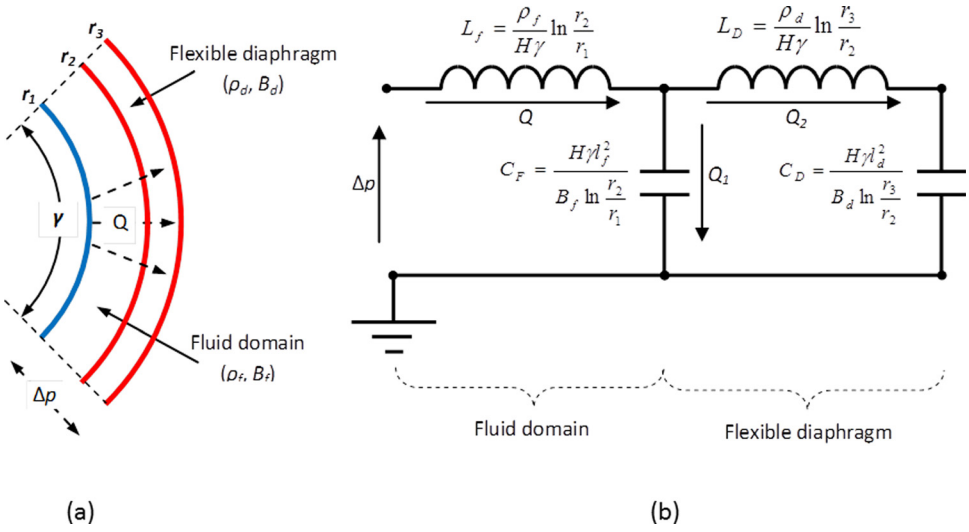

FIG. 2. (Color online) (a) Geometry and (b) analogous circuit of acoustic sector cavity coupled with flexible diaphragm.

Substituting Eqs. (12)–(15) into Eq. (16) and rearranging, results in the acoustic impedance Z_t for the two-material composite cavity system as follows:

$$Z_t = \frac{B_f}{sH\gamma}\left(\frac{s^2 \ln\frac{r_2}{r_1}}{c_f^2} + \frac{B_d\left(1+\frac{s^2 l_d^2}{c_d^2}\right)\ln\frac{r_3}{r_2}}{B_f l_d^2 + B_d l_f^2\left(1+\frac{s^2 l_d^2}{c_d^2}\right)}\right). \tag{17}$$

Referring to Euler's Equation for acoustic domains,

$$\Delta p = \int_{r_1}^{r_3} dp = \int_{r_1}^{r_3} \frac{\rho_{\text{eff}}}{A(r)}\frac{dQ}{dt}dr = \frac{\rho_{\text{eff}}}{H\gamma}\frac{dQ}{dt}\ln\frac{r_3}{r_1},$$

and applying Laplace transformation, the effective dynamic density of the composite domain ρ_{eff} is eventually defined as

$$\rho_{\text{eff}} = \frac{B_f}{s^2 \ln\frac{r_3}{r_1}}\left(\frac{s^2 \ln\frac{r_2}{r_1}}{c_f^2} + \frac{B_d\left(1+\frac{s^2 l_d^2}{c_d^2}\right)\ln\frac{r_2}{r_3}}{B_f l_d^2 + B_d l_f^2\left(1+\frac{s^2 l_d^2}{c_d^2}\right)}\right). \tag{18}$$

Equation (18) reveals that the effective dynamic density for the composite material is negative and approaches that of the fluid domain at higher frequencies as shown in Fig. 3, where the fluid domain modeled was water ($\rho_f = 1000\,\text{kg/m}^3$, $B_f = 2.25 \times 10^9\,\text{Pa}$) coupled with a thin steel diaphragm ($\rho_d = 7800\,\text{kg/m}^3$, $B_d = 210 \times 10^9\,\text{Pa}$), which is typical behavior as reported by Baz.[26] Due to the dependence of the effective dynamic density, for such composite system, on the effective bulk modulus of the two-material homogenized system, it is targeted to develop a methodology of varying the bulk modulus of the flexible diaphragm in order to yield a "programmable" effective density of the homogenized system that can assume any prescribed value over a wide frequency range.

E. Dynamic density for sector acoustic cavity coupled with piezoelectric diaphragm

Consider the sector acoustic cavity coupled with a flexible diaphragm shown in Fig. 2(a), where the flexible diaphragm is replaced with a piezoelectric one. The basic constitutive equation for a piezoelectric material is given by

$$\begin{Bmatrix} S \\ D \end{Bmatrix} = \begin{bmatrix} s^E & d \\ d & \varepsilon \end{bmatrix}\begin{Bmatrix} T \\ E \end{Bmatrix}, \tag{19}$$

where S = strain, D = electric displacement, T = stress, E = electrical field, s^E = compliance, d = piezoelectric strain coefficient, and ε = permittivity of piezoelectric material. Equation (19) can be rewritten as

$$\begin{Bmatrix} \Delta\text{Vol} \\ q \end{Bmatrix} = \begin{bmatrix} C_D & d_A \\ d_A & 1/z_p s \end{bmatrix}\begin{Bmatrix} \Delta p_p \\ V_p \end{Bmatrix}, \tag{20}$$

where ΔVol = change in diaphragm volume, q = electrical charge, Δp_p and V_p are the acoustic pressure and voltage difference across the piezoelectric diaphragm. A similar derivation was presented by Prasad *et al.*[28] However, in the current derivation the electrical free capacitance of the piezoelectric material Z_p presented by Prasad *et al.* is replaced with an equivalent circuit that comprises the capacitance of the piezoelectric diaphragm C_p combined with *in-parallel* inductance

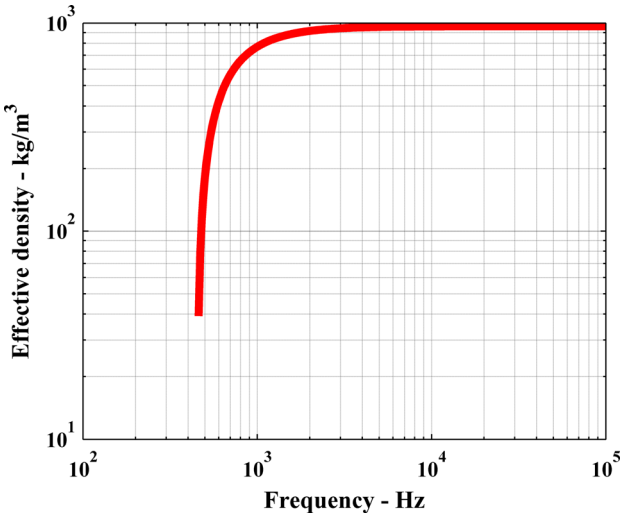

FIG. 3. (Color online) Dynamic effective density for an acoustic sector cavity coupled with flexible diaphragm.

L_p and *in-series* capacitance C_s to allow for stability measures of the active element as will be demonstrated later,

$$Z_p = \frac{L_p s}{1 + \frac{L_p C_p C_s s^2}{C_p + C_s}}. \tag{21}$$

1. Calculation of C_p

To calculate the value for C_p, the electric field E across the piezoelectric sector element must be calculated. Hence, a Gaussian cylinder of radius r and thickness H is constructed ($\oint E\,dA = E\oint dA$). The ends of the cylinder are normal to the field and do not contribute to the integral. The only part that contributes to the electric field is the sector confined by the angle γ, which area is calculated as $\oint dA = \gamma r H$. As the integral form of Gauss law is defined as $\oint E\,dA = \sum q/\varepsilon$, where $\sum q$ (or simply q) is the total charge on the curved sector element ($q = \varepsilon E \gamma r H$), moving a positive test charge between the sector boundary surfaces, ranging from inner radius r_2 to outer radius r_3, requires applied work equal to the change in the electric potential energy $\Delta EPE = \int_{r_2}^{r_3} F dr = \int_{r_2}^{r_3} qE dr = qV_p$, where $V_p = \int_{r_2}^{r_3} (q/\varepsilon\gamma r H) dr = (q/\varepsilon\gamma r H)\ln(r_3/r_2)$, is the potential difference between the two piezoelectric sector sides, yielding an expression for $C_p = \varepsilon\gamma H/\ln(r_3/r_2)$.

2. Calculation of C_D and d_A

To calculate the value for C_D and d_A as in Eq. (20), the effect of the electric-mechanical coupling in the piezoelectric materials on the total potential energy stored in the piezoelectric sector element is calculated using Eq. (6), where, F in this case is the elastic force inside the sector cavity due to both the mechanical strain and the electrical field and ΔPE is the change in potential energy such that $\int_{r_1}^{r_2} A(r) T dr = \Delta p \Delta \mathrm{Vol}$. Using the expression for the total stress inside the piezoelectric sector $T = (S - dE)/s^E$ extracted from Eq. (19) and replacing s^E with $1/B_d$ (bulk modulus of piezoelectric sector diaphragm), the acoustic pressure difference across the sector is calculated as

$$\frac{B_d}{\gamma H l_d^2}\int_{r_2}^{r_3} \frac{\Delta \mathrm{Vol}}{r} dr - \gamma H l_d d \int_{r_2}^{r_3} E dr = \Delta p_p. \tag{22}$$

Integrating Eq. (22) yields an expression for $\Delta p_p = (B_d/\gamma H l_d^2)\Delta \mathrm{Vol}\ln(r_3/r_2) + \gamma H l_d d V_p$, which can be rearranged to calculate the values of $C_D = (\gamma H l_d^2/B_d)\ln r_3/r_2$ and $d_A = d_\gamma H l_d/\ln(r_3/r_2)$. The electrical circuit analogous to the coupled fluid-piezoelectric sector cavities is hence as illustrated in Fig. 4. The parameter $\phi = -d_A/C_D\phi$, also called the transformer turns ratio in the equivalent circuit representation, is the electroacoustic transduction coefficient.

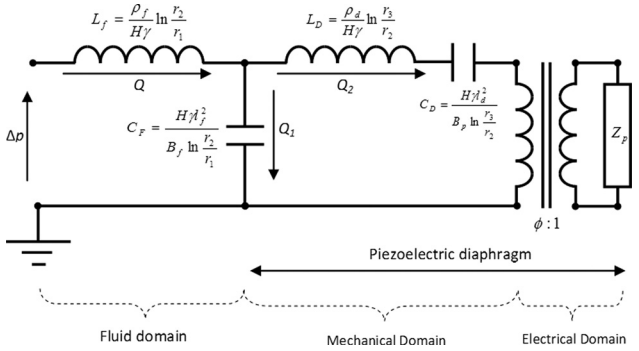

FIG. 4. Analogous circuit of an acoustic fluid domain coupled with open-loop piezoelectric diaphragm.

Using the piezoelectric diaphragm as a self-sensing actuator, then the second row of Eq. (20) gives, for a short-circuit piezosensor, the electric charges in the piezoelectric diaphragm $q = d_A \Delta p_p$. In which case, the voltage V_p applied to the diaphragm can be generated by a direct feedback of the charge q such that $V_p = -G d_A \Delta p_p$, where G = feedback gain. Then, the first row of Eq. (20) yields

$$\Delta \mathrm{Vol} = (C_D - d_A^2 G)\Delta p_p = C_{DC}\Delta p_p, \tag{23}$$

where C_{DC} = closed-loop compliance of the piezoelectric diaphragm. Figure 5 displays the corresponding electrical circuit analogous of the acoustic cavity integrated with a closed-loop piezoelectric diaphragm characterized with overall impedance given by

$$Z_t = \frac{(Z_p' + Z_{CDC} + Z_{LD})Z_{CF}}{Z_p' + Z_{CDC} + Z_{LD} + Z_{CF}} + Z_{LF}. \tag{24}$$

Recalling the identities defined in Eqs. (12)–(15), and noting that $B_p = (H\gamma l_d^2/C_{DC})\ln r_3/r_2$, the total impedance Z_t and the effective density ρ_{eff} of the coupled composite sector cavity may be expressed as

$$Z_t = \frac{B_f \ln\frac{r_3}{r_2}\left(H l_d^2 s Z_p' \gamma + (B_p + \rho_d l_d^2 s^2)\ln\frac{r_3}{r_2}\right) + s^2\rho_f \ln\frac{r_2}{r_1}\left(H l_d^2 l_f^2 s Z_p' \gamma + (B_f l_d^2 + B_d l_f^2 + \rho_d l_d^2 l_f^2 s^2)\ln\frac{r_3}{r_2}\right)}{Hs\gamma\left(H l_d^2 l_f^2 s Z_p' \gamma + (B_f l_d^2 + B_d l_f^2 + \rho_d l_d^2 l_f^2 s^2)\ln\frac{r_3}{r_2}\right)}, \tag{25}$$

$$\rho_{\mathrm{eff}} = \frac{B_f \ln\frac{r_3}{r_2}\left(H l_d^2 s Z_p' \gamma + (B_p + \rho_d l_d^2 s^2)\ln\frac{r_3}{r_2} + s^2\rho_f \ln\frac{r_2}{r_1}\left(H l_d^2 l_f^2 s Z_p' \gamma + (B_f l_d^2 + B_d l_f^2 + \rho_d l_d^2 l_f^2 s^2)\ln\frac{r_3}{r_2}\right)\right.}{s^2\left(H l_d^2 l_f^2 s Z_p' \gamma + (B_f l_d^2 + B_d l_f^2 + \rho_d l_d^2 l_f^2 s^2)\ln\frac{r_3}{r_2}\right)\ln\frac{r_3}{r_1}}. \tag{26}$$

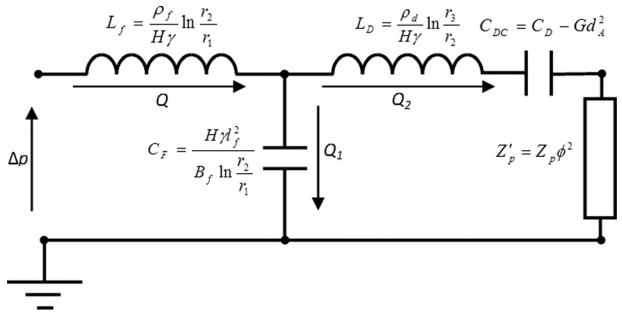

FIG. 5. Analogous circuit for an acoustic fluid domain coupled with closed-loop piezoelectric diaphragm.

After rearrangement of Eq. (26), the bulk modulus of the piezodiaphragm B_p and the control gain needed to realize specified value for ρ_{eff} can be represented as a frequency dependent function of Z'_p as follows:

$$B_p = s^2 l_d^2 \left(\frac{B_f \left(\rho_{\text{eff}} \ln \frac{r_3}{r_1} - \rho_f \ln \frac{r_2}{r_1} \right)}{l_f^2 s^2 \left(\rho_f \ln \frac{r_2}{r_1} - \rho_{\text{eff}} \ln \frac{r_3}{r_1} \right) + B_f \ln \frac{r_3}{r_2}} - \frac{HZ'_p \gamma}{\ln \frac{r_3}{r_2}} - \rho_d \right), \tag{27}$$

$$G = \frac{H\gamma l_d^2}{d_A^2 \ln \frac{r_3}{r_2}} \left(\frac{1}{B_d} - \frac{1}{B_p} \right). \tag{28}$$

A numerical simulation of a sector-shaped composite cavity using the developed model is developed and the frequency dependent piezoelectric bulk modulus B_p, feedback control gain G and resultant effective density ρ_{eff} for the composite system for target relative density values ($\rho_r = \rho_{\text{eff}}/\rho_f = 20$) and ($\rho_r = 0.05$) are presented in Fig. 6, which were developed using the values listed in Table I and specific values of $C_s = 5 \times 10^{-10}$ Farad and $L_P = 0.02$ H. It is important, however, to optimize the values of C_s and L_p to obtain the largest bandwidth with feasible control gain values. Hence, a sensitivity analysis is needed to determine the stability bandwidth of the piezodiaphragm without reaching a bucking state of the diaphragm material due to the applied control voltage.

III. CASCADING COMPOSITE CAVITIES WITH VARIOUS PROGRAMMABLE DENSITIES

In the previous section, a single cavity coupled with a piezoelectric diaphragm was considered. The effective dynamic density of the composite domain was proven to be controllable by varying the dynamic bulk modulus of the piezoelectric diaphragm to yield a frequency-dependent dynamic density as required. In order to expand the applicability of the introduced methodology, a set of cascading and coupled composite metamaterial cells are modeled such that each is programmed to yield different dynamic density value. This setup is very important in the path to realize

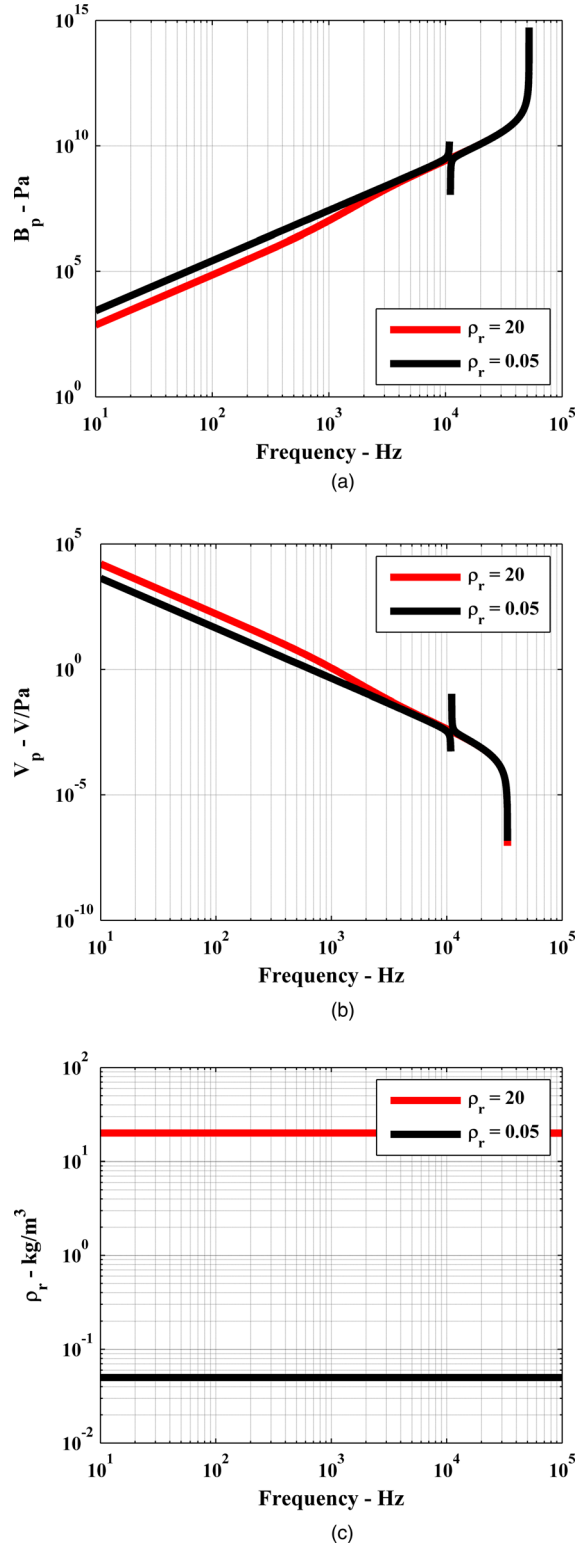

FIG. 6. (Color online) (a) Bulk modulus of piezodiaphragm, (b) control voltage, and (c) relative density for $\rho_r = 20$ and 0.05.

phenomena such as acoustic cloaking, where fluid layers circumscribing a solid cylinder, for example, can yield the cloaking phenomenon, provided that their densities and bulk modulus take a prescribed set of values as demonstrated by Cheng *et al.*[29]. The schematic presentation of the cascading cavity cells and the corresponding analogous electric circuits are as shown in Fig. 7.

TABLE 1. Parameters of acoustic cavity/piezodiaphragm system.

Parameter	Value
H	0.05 m
γ	$\pi/36$ rad
R_1	0.1 m
l_f	0.01 m
l_d	0.002 m
D	-170×10^{-12} m/V
ρ_f	1000 kg/m^3
ρ_d	7800 kg/m^3
B_f	2.25×10^9 Pa
B_d	48.31×10^9 Pa
ε_r	1750

In this system, the last cell represents the cell subject to external pressure excitation, while the first one is the end of the chain of the cascading cells. Due to the coupling nature of the cells, a recursive solution pattern has to be adopted in order to calculate the different values of the control gains $G_{(i)}$ needed to alter the effective bulk modulus of the piezoelectric diaphragms coupled to each cell $B_{p(i)}$ to ensure a prescribed set of effective densities within the cascading coupled cells.

The recursive approach starts with the first cell, which is coupled from one side only to the rest of the metamaterial domain. Using the electrical analogy, the overall impedance $Z_{(1)}$ of this cell can be calculated as a function of the piezoelectric diaphragm Bulk modulus $B_{p(1)}$ and the required effective density $\rho_{\text{eff}(1)}$, as given by Eqs. (27) and (28). Once calculated, this impedance is shunted to the circuit representing the rest of the chain. Hence the second cell, loaded with the impedance of the first cell, is now the end of the chain, and is coupled to the rest of the cells from one side only. Again using the electrical analogy, the overall impedance $Z_{(2)}$ of the first two cells can be calculated as a function of the piezoelectric diaphragm bulk modulus $B_{p(2)}$ and the required density ratio for this cell $\rho_{\text{eff}(2)}$. Following the same logic, the gains $G_{(i)}$ for the different cells that would yield the prescribed set of effective density values can be obtained. The impedance of the ith cell and consequently the effective density and the bulk modulus of the piezoelectric diaphragm for the ith cell are hence given by

$$Z_{(i)} = \frac{\left(\left(\frac{Z_{(i-1)}\left(Z_{CDC(i)} + Z'_{p(i)}\right)}{Z_{(i-1)} + Z_{CDC(i)} + Z'_{p(i)}}\right) + Z_{LD(i)}\right) Z_{CF(i)}}{\left(\frac{Z_{(i-1)}\left(Z_{CDC(i)} + Z'_{p(i)}\right)}{Z_{(i-1)} + Z_{CDC(i)} + Z'_{p(i)}}\right) + Z_{LD(i)} + Z_{CF(i)}} + Z_{LF(i)}, \tag{29}$$

$$\rho_{\text{eff}(i)} = Z_{(i)} \frac{H\gamma}{s \ln \frac{r_{3(i)}}{r_{l(i)}}}, \tag{30}$$

$$B_{p(i)} = \frac{B_f \ln \frac{r_{3(i)}}{r_{2(i)}} \left(Hl_d^2 s Z'_{p(i)} \gamma + (B_p + \rho_d l_d^2 s^2) \ln \frac{r_{3(i)}}{r_{2(i)}}\right) + s^2 \rho_f \ln \frac{r_{2(i)}}{r_{1(i)}} \left(Hl_d^2 l_f^2 s Z'_{p(i)} \gamma + (B_f l_d^2 + B_d l_f^2 + \rho_d l_d^2 l_f^2 s^2) \ln \frac{r_{3(i)}}{r_{2(i)}}\right)}{s^2 \left(Hl_d^2 l_f^2 s Z'_{p(i)} \gamma + (B_f l_d^2 + B_d l_f^2 + \rho_d l_d^2 l_f^2 s^2) \ln \frac{r_{3(i)}}{r_{2(i)}}\right) \ln \frac{r_{3(i)}}{r_{1(i)}}}. \tag{31}$$

The developed model for a system of four cascading cells has been numerically verified with targeted relative density values $\rho_r = 20$, 0.05, 12, and 0.15. The frequency-dependent bulk modulus and corresponding control voltages are as plotted in Fig. 8.

IV. SENSITIVITY ANALYSIS AND PIEZOELECTRIC STABILITY

As mentioned earlier a shunted inductance *in-parallel* L_p and capacitance *in-series* C_s are added to the piezoelectric sector element to eliminate the instability that might occur due to the applied control voltage to achieve the targeted relative density values. This instability might show up in the form of negative value of the piezoelectric bulk modulus indicating a state of buckling. This approach has proven to be efficient as reported by Akl and Baz.[27] However, adding these two elements introduces an additional pole in the frequency spectrum of the piezoelectric sector bulk modulus. It is therefore the objective of this section to study the effect of the added components on the operating bandwidth of the newly developed composite acoustic metamaterial. The expression for the bulk modulus B_p presented in Eq. (27) can hence be rewritten as

$$B_p = -\rho_d l_d^2 s^2 - \frac{(C_p + C_s) H l_d^2 s^2 \lambda \phi^2}{(C_p + C_s + C_p C_s L_p s^2) \ln \frac{r_3}{r_2}} + \frac{B_f l_d^2 s^2 \left(\rho_f \ln \frac{r_2}{r_1} - \rho_{eff} \ln \frac{r_3}{r_1}\right)}{l_f^2 s^2 \left(\rho_f \ln \frac{r_2}{r_1} - \rho_{eff} \ln \frac{r_3}{r_1}\right) + B_f \ln \frac{r_3}{r_2}}, \tag{32}$$

which indicates the existence of two singularities; the first is dependent on the cavity dimensions and properties and the other is totally dependent on the electric components of the

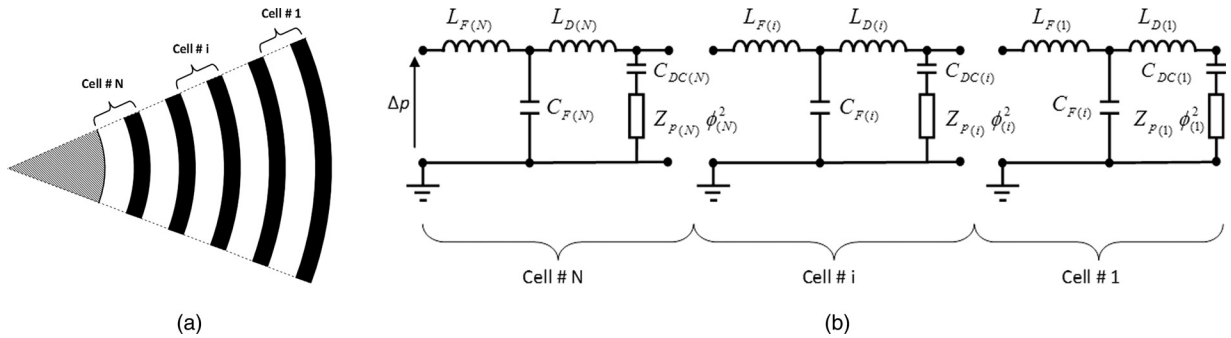

FIG. 7. (a) Schematic and (b) analogous circuit for a set of N cascading and coupled cells.

piezoelectric sector elements combined with the added inductance and capacitance. The singularities (resonant frequencies f_1 and f_2) occur at

$$f_1 = \frac{1}{2\pi l_f}\sqrt{\frac{B_f \ln\frac{r_3}{r_2}}{\rho_f \ln\frac{r_2}{r_1} - \rho_{\text{eff}} \ln\frac{r_3}{r_1}}}, \tag{33}$$

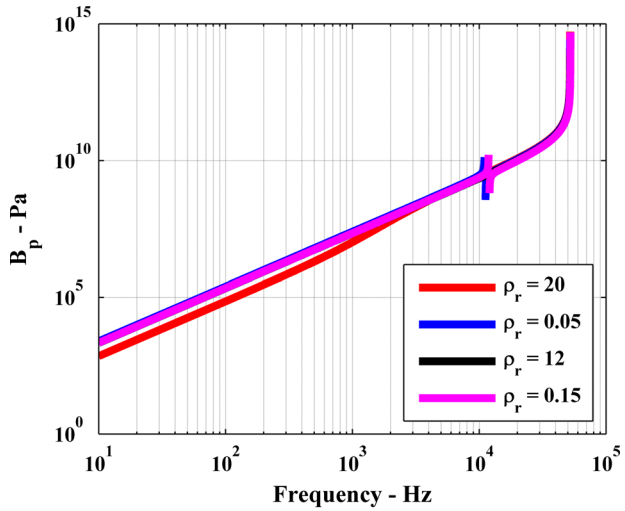

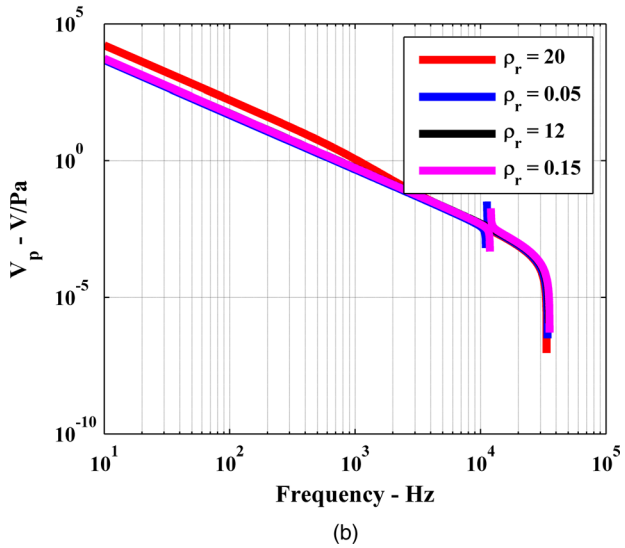

FIG. 8. (Color online) (a) Piezodiaphragm bulk modulus and (b) control voltage for four cascading and coupled cells targeting relative density values $\rho_r = 20$, 0.05, 12, and 0.15.

$$f_2 = \frac{1}{2\pi}\sqrt{\frac{C_p + C_s}{C_p C_s L_p}}. \tag{34}$$

Figure 9 illustrates a contour plot for the resonance frequency of the electrical components of the acoustic metamaterial as a function of C_s and L_p. In the design process, this frequency has to be taken into consideration to select the values of C_s and L_p connected to C_p to resonate at a frequency away from the targeted operating bandwidth. However, one should be cautious reducing the values of L_p and C_s as this significantly affects the control voltage needed, especially at lower frequencies. Figure 10 shows the effect of L_p on V_P. C_s has shown no significant effect on the control voltage needed to achieve a targeted relative density.

V. CONCLUSIONS

A new class of one-dimensional acoustic metamaterial with controllable density, developed in cylindrical coordinate system is presented. The proposed metamaterial is designed to take a circular sector shape to allow for coupling and/or integrating with irregular shaped objects. The effective density of the composite metamaterial has been theoretically proven to be controllable and thus any required value of the effective density can be achieved along a very wide

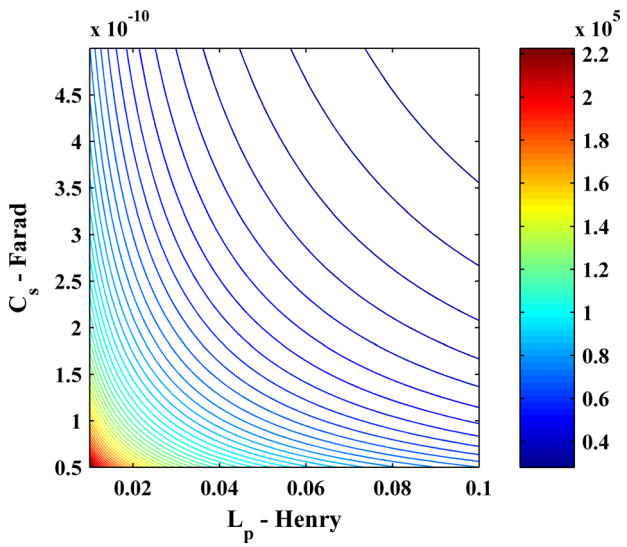

FIG. 9. (Color online) Electrical components resonance frequency as a function of C_s and L_p.

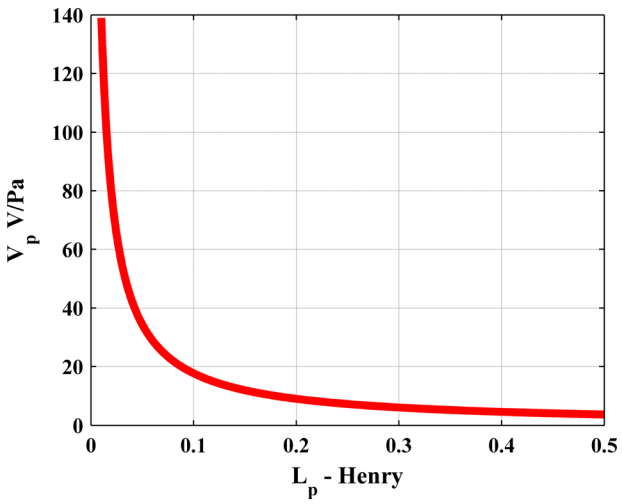

FIG. 10. (Color online) Effect of L_P on the control voltage V_p.

frequency spectrum. The theoretical analysis of this class of active acoustic metamaterials is presented for an array of water cavities separated by piezoelectric boundaries using a lumped-parameter modeling approach. The same model is also applied for a set of cascading coupled cells. A sensitivity and stability analysis is conducted to optimize the piezoelectric electric parameters to prevent the instability that might occur due to the applied control voltage. A natural extension of this work is to include active control capabilities to tailor the bulk modulus distribution of the proposed metamaterial configuration.

ACKNOWLEDGMENTS

This work has been funded by a grant from the Office of Naval Research (N000140910038). Special thanks are due to Dr. Kam Ng and Dr. Scott Hassan, the technical monitors, for their invaluable inputs and comments.

[1]M. Lapine, "The age of metamaterials," Metamaterials **1**, 1 (2007).
[2]E. Shamonina and L. Solymar, "Matematerials: how the subject started," Metamaterials **1**, 12–18 (2007).
[3]M. Gil, J. Bonache, and F. Martin, "Metamaterial filters: A review," Metamaterials, **2**(4), 186–197 (2008).
[4]N. Engheta and R. Ziolkowski, *Metamaterials: Physics and Engineering Explorations* (Wiley, New York, 2006), p. 414.
[5]J. B. Pendry, "Negative refraction makes a perfect lens," Phys. Rev. Lett. **85**(18), 3966–3969 (2000).
[6]J. B. Pendry, D. Schurig, and D. R. Smith, "Controlling electromagnetic fields," Science **312**(5781), 1780–1782 (2006).
[7]S. A. Cummer, B. Popa, D. Schurig, D. R. Smith, and J. B. Pendry, "Full-wave simulations of electromagnetic cloaking structures," Phys. Rev. E **74**, 36621 (2006).
[8]Q. Wu, K. Zhang, F. Meng, and L. Li, "Material parameters characterization for arbitrary N- sided regular polygonal invisible cloak," J. Phys. D **42**(3), 35408–35414 (2009).
[9]S. Guenneau, A. Movchan, G. Pétursson, and A. Ramakrishna, "Acoustic metamaterials for sound focusing and confinement," New J. Phys. **9**(399), 1367–2630 (2007).
[10]S. A. Cummer and D. Schurig, "One path to acoustic cloaking," New J. Phys. **9**, 45 (2007).
[11]A. N. Norris, "Acoustic cloaking theory," Proc. R. Soc. London, Ser. A **464**(2097), 2411–2434 (2008).
[12]L. Jensen, and C. T. Chan, "Double negative acoustic metamaterial." Phys. Rev. E **70**(5), 55602 (2004).
[13]Y. Ding, Z. Liu, C. Qiu, and J. Shi, "Metamaterial with simultaneously negative bulk modulus and mass density," Phys. Rev. Lett. **99**(9), 93904 (2007).
[14]S. H. Lee, C. M. Park, Y. M. Seo, Z. G. Wang, and C. K. Kim, "Acoustic metamaterial with negative modulus," J. Phys.: Condens. Matter, **21**, 175704 (2009).
[15]S. Choi and Y. Kim, "Sound wave propagation in a membrane-duct," J. Acoust. Soc. Am. **112**, 1749–1752 (2002).
[16]Y. H. Chiu, L. Cheng, and L. Huang, "Drum-like silencers using magnetic forces in a pressurized cavity," J. Sound Vib. **297**, 895–915 (2006).
[17]W. Akl and A. Baz, "Configuration of active acoustic metamaterial with programmable bulk modulus," Proc. SPIE **7643**, 76432K (2010).
[18]F. Cavera, L. Sanchis, J. Perez, R. Sala, C. Rubio, and F. Meseguer, "Refractive acoustic devices for airborne sound," Phys. Rev. Lett. **88**(2), 23902 (2001).
[19]A. Krokhin, J. Arriaga, and L. Gumen, "Speed of sound in periodic elastic composites," Phys. Rev. Lett. **91**(26), 264302 (2003).
[20]D. Torrent, and J. Sanchez-Dehesa, "Acoustic metamaterials for new two-dimensional sonic devices," New J. Phys. **9**, 323 (2007).
[21]C. T. Chan, L. I. Jensen, and K. H. Fung, "On extending the concept of double negativity to acoustic waves," J. Zhejiang Univ., Sci. A **7**(1), 24–28 (2006).
[22]G. W. Milton and J. R. Willis, "On modifications of Newton's second law and linear continuum elastodynamics," Proc. R. Soc. London, Ser. A **463**(2079), 855–880 (2006).
[23]S. Yao, X. Zhou, and G. Hu, "Experimental study on negative effective mass in a 1D mass- spring system," New J. Phys. **10**, 43020 (2008).
[24]H. Huang, C. Sun, and G. Huang, "On the negative effective mass density in acoustic metamaterials," Int. J. Eng. Sci. **47**(4), 610–617 (2009).
[25]A. Baz, "An active acoustic metamaterial with tunable effective density," J. Vib. Acoust. **132**(4), 041011 (2010).
[26]A. Baz, "The structure of an active acoustic metamaterial with tunable effective density," New J. Phys. **11**, 1230102009 (2009).
[27]W. Akl and A. Baz, "Multi-cell active acoustic metamaterial with programmable bulk modulus," J. Intell. Mater. Syst. Struct. **21**, 541–556 (2010).
[28]S. A. Prasad, Q. Gallas, S. Horowitz, B. Homeijer, B. V. Sankar, L. N. Cattafesta, and M. Sheplak, "Analytical electroacoustic model of a piezoelectric composite circular plate," AIAA J. **44**(10), 2311–2318 (2006).
[29]Y. Cheng, F. Yang, J. Y. Xu, and X. J. Liu, "A multilayer structured acoustic cloak with homogeneous isotropic materials," Appl. Phys. Lett. **92**, 151913 (2008).